Response to Reviewer 2 Comments

Manuscript ID: catalysts-2013897

Title: Annealing and plasma effects on the structural and photocatalytic properties of TiO2 fibers produced by electrospinning

Point 1: The paper contains some grammatical errors and typo mistakes that should be corrected.

Response 1: Thank you for your valuable and thoughtful comments. All the authors of this manuscript have carefully and repeatedly checked and improved the English writing in the revised manuscript. Pr. Antoine Goullet and English major teachers are invited to modify the grammar and expression of the full manuscript.

Point 2: The Abstract part should be more concise. It is too long. The abstract should clearly inform the important findings of the present study as well as some qualitative and quantitative results should be provided.

Response 2: Thanks the reviewer. The abstract has been modified in the revised manuscript as follows:

In this study, the combined method of heat treatment and plasma surface modification is used to improve the nanostructures and photocatalytic activity of electrospinning TiO_2 fibers. Based on the tuning effect of the annealing temperature from 500 to 800 °C, further improvement by generating the H_2 radiofrequency plasma reaction on the fiber surface is investigated. It is found that the anatase-rutile phase transition starts to occur at around 700 °C which is higher than the common temperature of TiO_2. The interfacial effect is generated by the symbiosis relationship between these two phases in the fibers which can enhance the photocatalytic activity since the anatase-rutile heterojunction in the mixed-phase TiO_2 has been formed. The dramatically arise of oxygen vacancies on the fiber surface are created by the H_2 plasma, this leads to the number of trapped electrons increases and results in an accelerated separation of photogenerated electrons and holes. Therefore, the photocatalytic mechanism including anatase-rutile heterojunction and TiO_2 fiber band structure containing oxygen vacancies is predicted. The degradation rate can be significant enhanced by increasing the annealing temperature until 700 °C, and about 1.5 times that of untreated fiber can be further improved after surface H_2 plasma treatment.

Point 3: The introduction part can be further improved. The authors are suggested to include recent references in the introduction part about previous studies performed on TiO2 nanomaterials.

Response 3: We reviewed some literatures and sorted out the related research works made by other authors. And the state-of-the-art has been improved as follows:

In view of the advantages and disadvantages of TiO_2, some scholars have made researches concerning the further improvement of its photocatalytic performance. It has been found that the formation of heterojunction structures on the surface can accelerate the separation of photogenerated electrons and holes, thus improving the photocatalytic efficiency [10-11]. Abraham et al. [12] prepared W^{6+}/TiO_2 heterojunctions by sol-gel method, the produced sample is spherical shape with uniform particle distribution. The degradation effect of Congo red was up to 86 %. Doping of metals (Bi, Mg, etc.) can also be used to make a positive effect on the improvement of photocatalytic efficiency [13-16]. Jung et al. [17] doped europium in TiO_2 by liquid plasma. It can be observed that the treated TiO_2 is composed of many irregular nanoparticles stacked together. The degradation rate

of acetyl salicylic acid reached 0.00148 min^{-1}. In the literature, it is known that plasma technology can produce defects such as oxygen vacancies and accelerate the separation of photogenerated electrons from holes. It also contributes to the improvement of photocatalytic efficiency [18-19]. Irala et al. [20] used nitrogen plasma to treat the TiO_2 film grown on carbon steel substrate, which improved the photocatalytic performance. After treatment, TiO_2 was attached in granular form. The degradation rate of methyl blue reached 0.009 min^{-1}, 1.3 times of that before treatment.

However, people also have to face the problem in practical applications since the powder recovery is difficult, and it is easy to cause secondary pollution. Therefore, it is of great significance to fix the semiconductor photocatalyst on the carrier. Carriers such as fibers, porous nickel foam, stainless steel mesh and porous sponge are highly valued because of their large comparative area and skeleton-like three-dimensional network structure. Fiber is widely used because of its large specific surface area and convenient recycling. Calisir et al. [21] prepared nitrogen-doped TiO_2 fibers through centrifugal spinning and calcination processes. The treated fibers showed a hollow shape and increased specific surface area, while there is little change in grain size and the band gap was reduced to 3.01 eV. The degradation efficiency of methylene blue was still 94.66% after three cycles of experiments. Zhang et al. [22] prepared a kind of glass hollow TiO_2 fiber film by dip coating and calcination. As the heating rate decreases, more holes appear and the specific surface area increases. After treatment, the degradation rate of methylene blue reached 93 %. It was 2.9 times higher than that before treatment. Li et al. [23] prepared Fe-doped TiO_2 fibers by hydrothermal method. Microscopic observation shows that the treated fibers exhibit needle-like morphologies. Lattice distortion occurs as Fe ions are doped. The separation speed of electron and hole is accelerated, which has a positive effect on the improvement of photocatalytic efficiency. After doping, the degradation ability of methylene blue reached 99.9%.

In recent years, the increasing requirements for material properties have greatly promoted the development of material surface modification technology. Plasma technology as a green, cheap and simple method has attracted extensive attention [24]. The plasma process is different from the general treatment method. The treatment system is dominated by charged particles and affected by external electric, magnetic and electromagnetic fields [25]. The treatment method has the characteristics of no influence on matrix performance, high efficiency, energy saving and environmental protection, simple process and so on [26]. Therefore, plasma modification can effectively improve the physicochemical properties of semiconductor photocatalysts.

In this study, the TiO_2 fiber prepared by electrospinning technology is modified by heat treatment combined with plasma regulation [27], so that its crystal phase and interfacial structures can maximize the improvement of photocatalytic performance. The effects of different heat treatment temperatures and plasma modification on micro/nano structure, optical and photocatalytic activity of TiO_2 fibers are analyzed, and the mechanism of photocatalytic degradation of organic compounds is predicted.

Point 4: Also, there are many studies in the literature about TiO2 fibers, and their structural, morphological, physical and photocatalytic properties are widely discussed. Important studies should be reported in the Introduction part, and a comparison of the current study with the previously published one could be performed in the results and discussion part.

Response 4: The authors would like to thank the reviewer for the suggestion. For this point, we have made improvements in the introduction part and discussion part (the end of this article), and the revised results are as follows:

Introduction section:

However, people also have to face the problem in practical applications since the powder recovery is difficult, and it is easy to cause secondary pollution. Therefore, it is of great significance to fix the semiconductor photocatalyst on the carrier. Carriers such as fibers, porous nickel foam, stainless steel mesh and porous sponge are highly valued because of their large comparative area and skeleton-like three-dimensional network structure. Fiber is widely used because of its large specific surface area and convenient recycling. Calisir et al. [21] prepared nitrogen-doped TiO_2 fibers through centrifugal spinning and calcination processes. The treated fibers showed a hollow shape and increased specific surface area, while there is little change in grain size and the band gap was reduced to 3.01 eV. The

degradation efficiency of methylene blue was still 94.66% after three cycles of experiments. Zhang et al. [22] prepared a kind of glass hollow TiO_2 fiber film by dip coating and calcination. As the heating rate decreases, more holes appear and the specific surface area increases. After treatment, the degradation rate of methylene blue reached 93 %. It was 2.9 times higher than that before treatment. Li et al. [23] prepared Fe-doped TiO_2 fibers by hydrothermal method. Microscopic observation shows that the treated fibers exhibit needle-like morphologies. Lattice distortion occurs as Fe ions are doped. The separation speed of electron and hole is accelerated, which has a positive effect on the improvement of photocatalytic efficiency. After doping, the degradation ability of methylene blue reached 99.9%.

Results and discussion section:

The photocatalytic performance of the prepared fibers in this work is compared with the different forms of other authors, as shown in Table 4. It can be seen that the prepared fibers have better degradation efficiency relative to the recent literature review on TiO_2 photocatalysts.

Table 4 The recent literature review on TiO_2 and the comparison between their photocatalytic efficiency and the results in this work.

Methods	Photocatalysts type	Simulated pollutant	The degradation rate constant K value	Ref
Plasma spraying	Coating	Methylene blue	0.0014 min^{-1}	[57]
DBD	Coating	Methyl orange	0.0146 min^{-1}	[58]
Sol-gel method	Particles	Methyl red	0.0160 min^{-1}	[59]
Reactive plasma	Powder	Bacteria	0.0010 min^{-1}	[60]
Hydrothermal synthesis	Fiber	CO_2	0.0110min^{-1}	[61]
DBD	Coating	Methylene blue	0.0099 min^{-1}	[62]
*Electrospinning, calcination	Fiber	Methyl orange	0.0157 min^{-1}	/
*H_2 plasma treatment	Fiber	Methyl orange	0.0223 min^{-1}	/

(DBD: Dielectric Barrier Discharge; * Represents the photocatalysts synthesized in this study)

Point 5: Check symbols in different figures like the x-axis of Figure 5(a), symbols in XPS and FT-IR figures, etc...

Response 5: Thanks the reviewer. We have corrected these figures in the revised manuscript as follows:

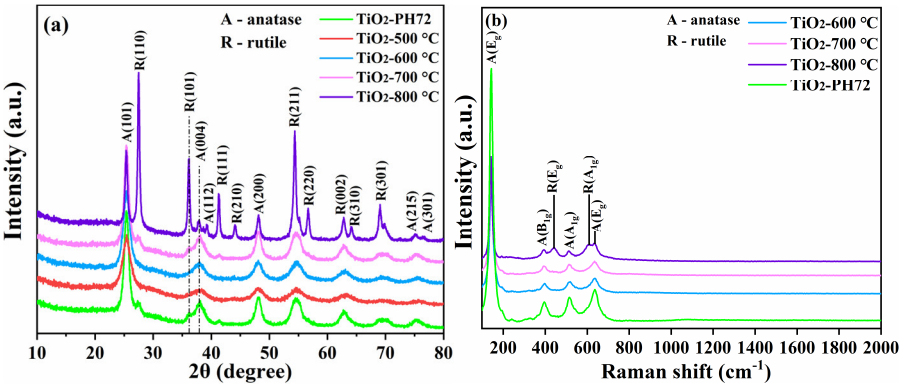

Figure 6

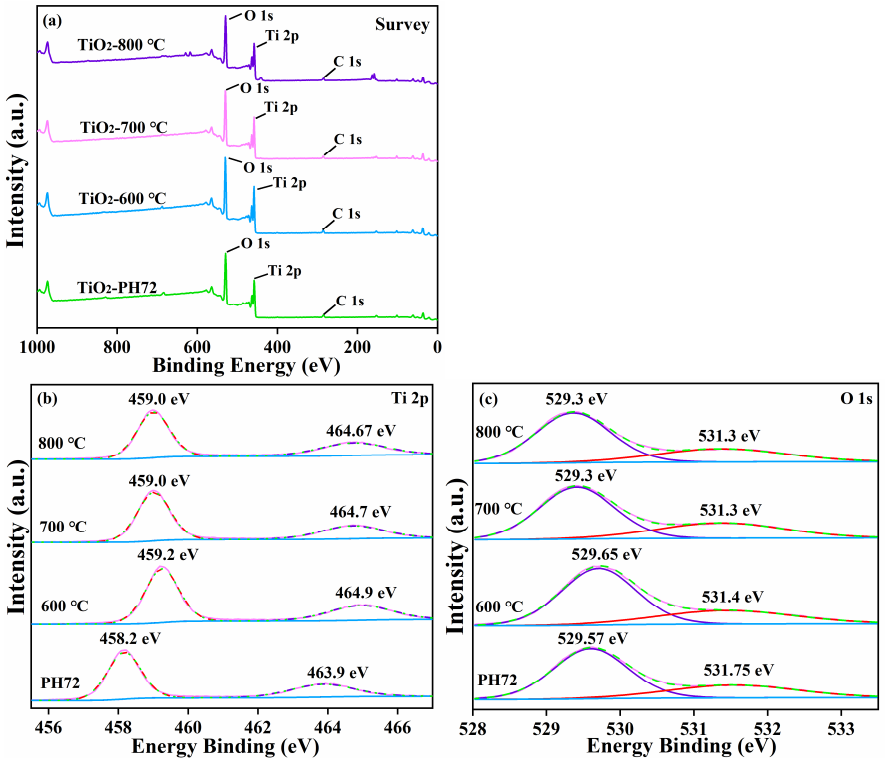

Figure 7

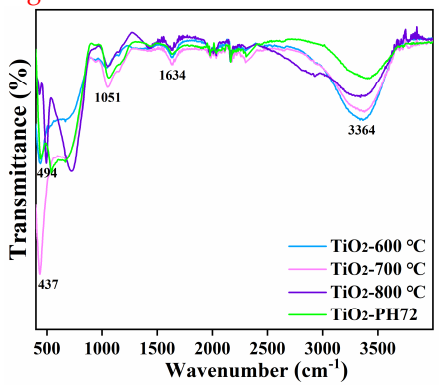

Figure 9

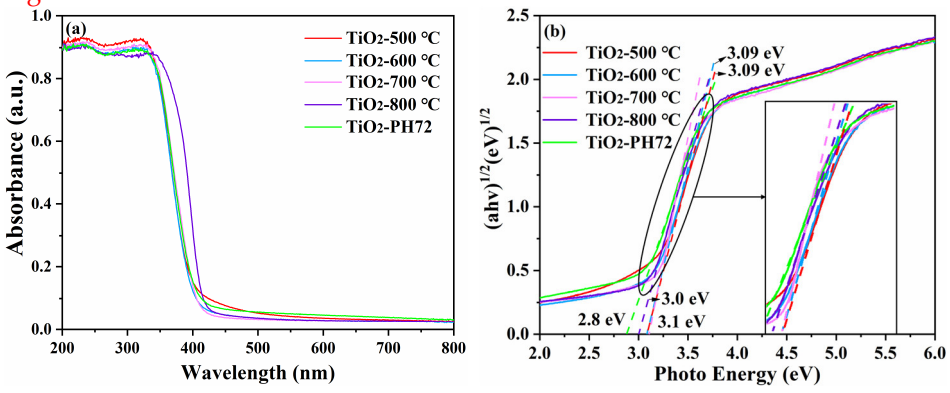

Figure 10

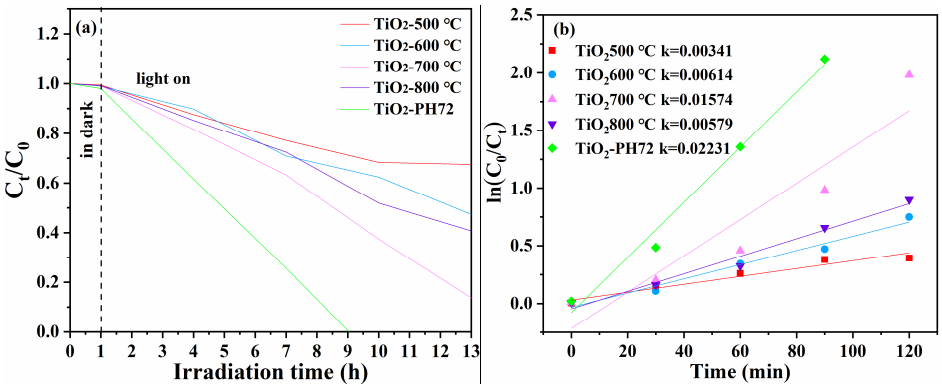

Figure 11

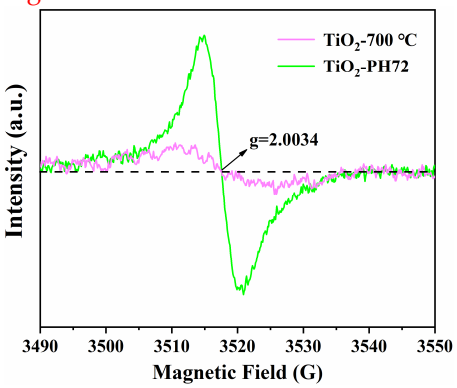

Figure 12

Point 6: The structural properties should be further discussed and improved. Some other important structural parameters should be determined and discussed like lattice parameters, crystallite size, etc. The plausible reasons for their variations should be provided accordingly.

Response 6: The authors would like to thank the reviewer for the suggestion. We have improved this part. They are shown below.

The formula $D=0.9\lambda/\beta\cos\theta$ [34] is used to calculate the grain diameter of each sample, where β is full width at half of the peak maximum (FWHM), λ is the wavelength of incident X-ray, θ is the diffraction Angle. The calculated values are shown in Table 1. It can be found that the grain size tends to increase with the increase of calcination temperature, while the gradual transition of anatase phase to rutile phase occurs [35]. There is a little change in grain size after H_2 plasma treatment. At 800 °C, the grain size changes obviously since the high calcination temperature, where the phase is almost rutile phase. At the same time, the formula $d^{-2} = (h^2+k^2)/a^2+l^2/c^2$ [36]was used to calculate the lattice constants a and c of each sample, the result is also shown in Table 1. It can be found that there is no crystal lattice changes at the different calcination temperatures [37].

Table 1 Grain size and lattice constant of all samples.

Sample	Grain size (nm)	Standard value of lattice parameter (Å)		Calculated lattice parameter (Å)	
		Anatase	Rutile	Anatase	Rutile
TiO_2-500 °C	55			a = 3.8536 c = 9.3607	/
TiO_2-600 °C	55.2			a = 3.7742 c = 9.4382	/
TiO_2-700 °C	56.2	a = 3.785 c = 9.514	a = 4.593 c = 2.959	a = 3.7892 c = 9.4010	a = 4.5815 c = 2.9422
TiO_2-800 °C	59.3			a = 3.7799 c = 9.4939	a = 4.5836 c = 2.9681

TiO_2-PH72	56.4	a = 3.7948 c = 9.3347	a = 4.5850 c = 2.9485

Point 7: Along with the presented SEM images, the authors should provide an analysis of grain size/diameter distribution.

Response 7: Thanks the reviewer. We have improved this part, the analysis of fiber diameter distribution has been added. The result is shown in Figure 2.

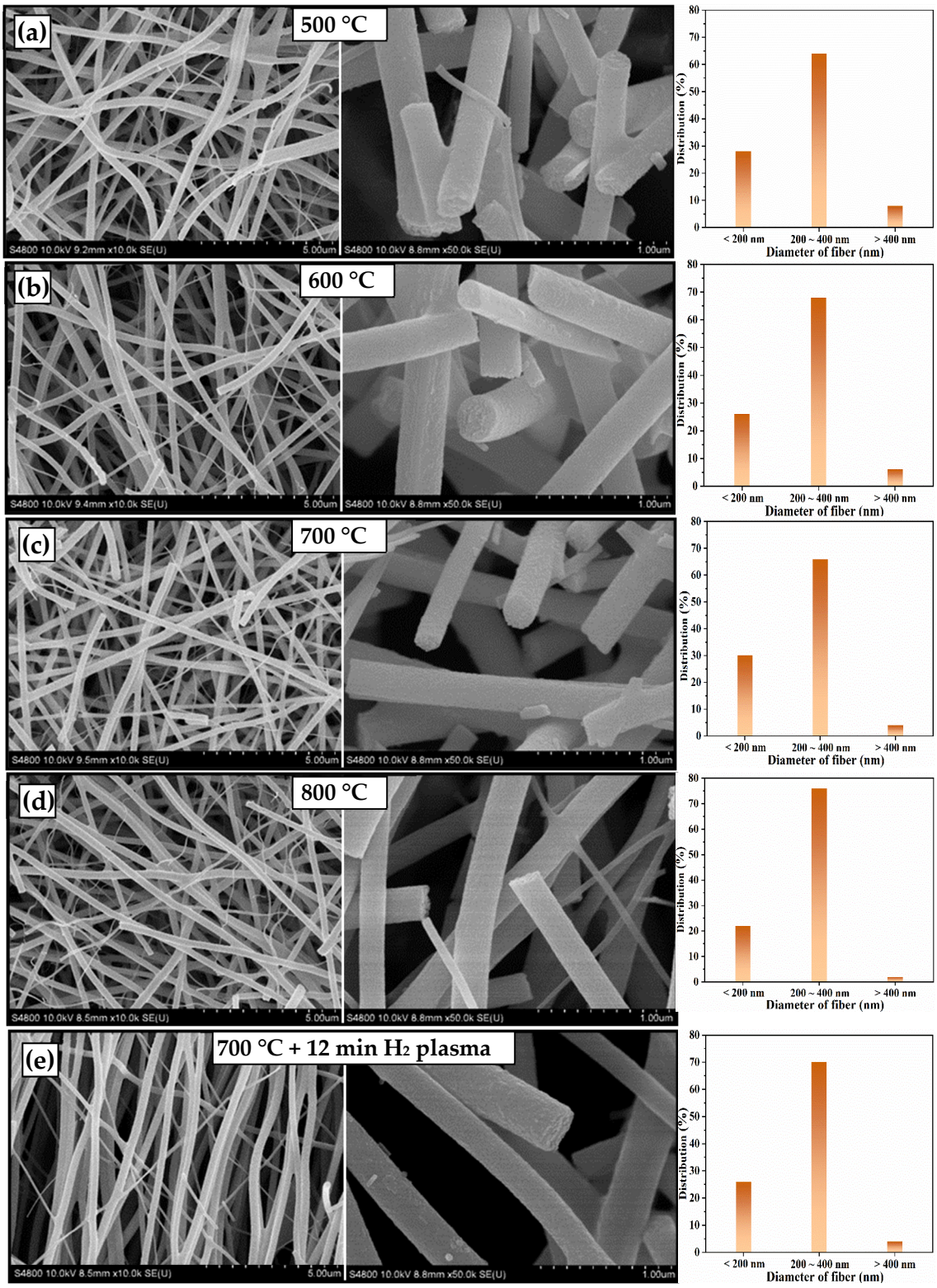

Point 8: The authors should add the EDX spectra and atomic percentages of different samples.

Response 8: The authors would like to thank the reviewer for the suggestion. We have added the EDX results of TiO_2-700 °C and TiO_2-PH72, while the XPS result concerning the atomic percentages of different samples was also fitted.

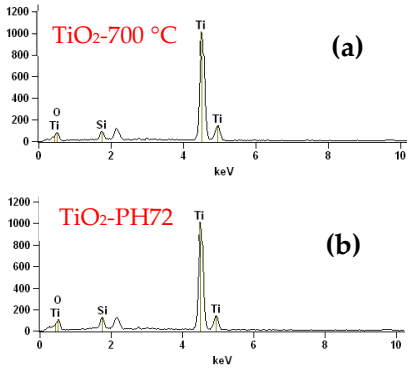

Figure 8. EDX images of (a) TiO_2-700 °C and (b) TiO_2-PH72 samples.

Figure 8 shows the EDX results of the fibers calcined at 700 °C and treated with H_2 plasma for 720 s. It is found that the main elements in the samples are Ti and O, which is consistent with the XPS results. And a small amount of Si presents in the samples may be caused by the contamination in the measurement process. For the element concentration, it is further analyzed by using the XPS measurement. Table 2 shows the elemental content of each sample, which is fitted from XPS spectra. The main elements in the sample are Ti and O, but the sum of the content of the two elements is less than 100%, which is caused by the introduction of C and other elements in the test. The content of oxygen atoms was observed to decrease after plasma treatment. This also proves the previous hypothesis of oxygen vacancy formation [43].

Table 2 Element content and O/Ti of each sample from XPS.

Samples	Element concentration		O/Ti
	O（%）	Ti（%）	
TiO_2-500 °C	62.90	32.12	1.96
TiO_2-600 °C	62.34	32.89	1.90
TiO_2-700 °C	61.83	33.12	1.87
TiO_2-800 °C	61.14	33.67	1.82
TiO_2-PH72	61.03	33.82	1.80

Point 9: Surface area is a very important parameter in the present case. Therefore, I suggest that the BET surface area measurement should be added if possible.

Response 9: The authors would like to thank the reviewer for the suggestion. We supplemented the BET test for the surface area measurement. The experimental results and analysis are as follows:

At the same time, BET test was performed on TiO_2-700 °C, TiO_2-800 °C and TiO_2-PH72 samples. It can be found that the specific surface area of the three samples is not different. It can also be observed from SEM images that the samples of TiO_2-700 °C, TiO_2-800 °C and TiO_2-PH72 are compact, with relatively smooth surfaces and no pores[30]. Therefore, the specific surface area is not the main factor to influence the photocatalytic performance in this study.

In this experimental study, the most important goal is to study the effect of oxygen vacancy and heterojunction structure on photocatalytic performance, and the change of specific surface area is not the focus of this paper. Thanks again for the reviewer's advice. In the following experiments, we will include the specific surface area factor as an important research direction.

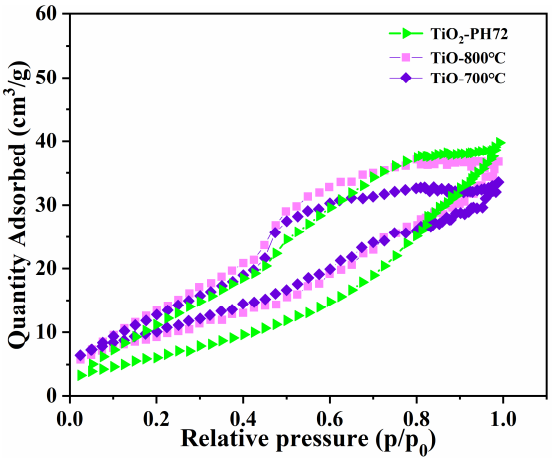

Figure 3 N_2 gas adsorption-desorption isotherm of the samples of TiO_2-700 °C, TiO_2-800 °C and TiO_2-PH72.

Point 10: In FT-IR spectra, there are additional vibration bonds that are not described. I think that it would be better to report all vibrational bonds and their positions in a table.

Response 10: We have studied all the corresponding vibration bonds in details, and reported all vibrational bonds and their positions in Table 3.

Table 3 The corresponding vibrational bonds in FTIR spectra.

Wavenumber (cm^{-1})	Vibrational bonds
437	Ti-O (Anatase)
494	Ti-O (Rutile)
717	Ti-O-Ti
1051	Ti-OH
1634	Polarity -OH
3364	Adsorbed water

Point 11: What does mean "taus diagram"? Do the authors mean "Tauc Plots"? It should be rechecked. The authors should provide some details on the determination of Eg values (not only giving references). Pls, provide an enlarged view of the Tauc plots (2.7 to 4 eV as maximum) to better determine the values of Eg. The discussion should be revised accordingly (there is a slight variation in Eg values).

Response 11: Thanks the reviewer. We have reviewed the questions raised by reviewer and changed "taus diagram" to "Tauc Plots". The details on the determination of Eg values have been provided. The X-axis of the Tauc Plots was enlarged, and the discussion was also revised. They are shown below.

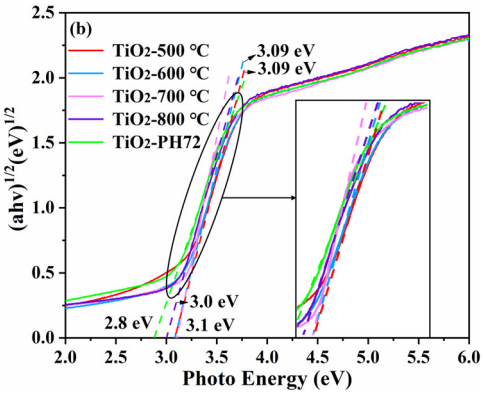

The following reference formula is often used to calculate the optical bandgap of photocatalysts: $(ahv)^{1/n} = C(hv-Eg)$, TiO_2 is an indirect bandgap semiconductor with index n = 2. The calculated band gap value is shown in Figure 10(b) [51-52]. For the samples of TiO_2-500 °C, TiO_2-600 °C and TiO_2-700 °C, the band gap value is roughly the same, which is around 3.1 eV since they are basically anatase phase. However, when the calcination temperature is higher than 700 °C, a large amount of anatase phase will change to rutile phase, which leads to a slight decrease in the band gap [53]. Furthermore, the fiber band gap value of TiO_2-PH72 is lower (~2.8 eV), this may be caused by the O defect formed during the plasma treatment process.

Point 12: Before the presentation of the photocatalytic degradation rate and kinetics of photocatalytic degradation, the graphs of absorbance vs wavenumbers at different durations should be presented.

Response 12: The authors would like to thank the reviewer for the suggestion. In our lab, the test of photocatalytic capacity was performed by using a UV-VIS photometer instrument. A photo of the instrument is displayed below. Due to the working permission of the instrument, we are not able to obtain the curves of absorbance spectra. We can only ensure that the transmittance is measured at a wavelength of 464 nm. In this way, the residual amount of methyl orange solution at different durations can also be detected. The detailed procedure for this measurement is described as follows:

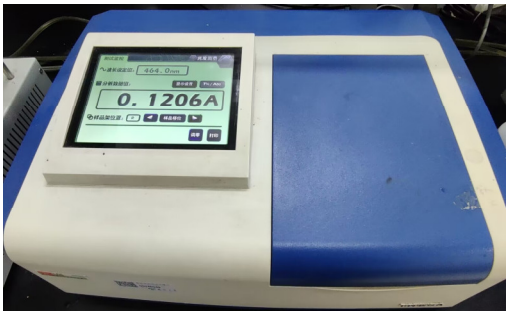

In the photocatalytic performance test, 0.02 g of photocatalyst was added to the photocatalytic reactor, and 100 ml of MO solution at a concentration of 25 ppm was added to obtain the mixed suspension. The suspension was placed in the dark, and the magnetic force of the device was turned on for 0.5 h. Then the suspension was irradiated with a 250 W xenon lamp to simulate the visible light irradiation environment. In the simulation of visible light environment, the temperature of the suspension was maintained at about 25 °C through an external cooling water pipe. The residual concentration of methyl orange was estimated by measuring the absorbance of methyl orange solution at the maximum absorption wavelength (464 nm) using a UV-vis spectrophotometer. Take 5 mL of methyl orange solution every 30 min., which was measured by the UV-vis photometer instrument after centrifugation. Before testing, the detection wavelength was adjusted to be located at 464 nm. After wavelength adjustment, deionized water was used for zero correction, then the obtained MO solution was tested, and the corresponding absorbance was recorded. The formula C_t/C_0 was used to calculate the residual concentration of methyl orange. Where C_t represents the absorbance of methyl orange at the measurement time, and C_0 represents the original absorbance of methyl orange before irradiation. C_t/C_0 was used to represent the degradation efficiency of the photocatalyst and to quantify its photocatalytic performance.

Point 13: Compare the photocatalytic results of the current samples with those for TiO2 (nano/micro)-fibers as well as other shaped nanomaterials.

Response 13: The authors would like to thank the reviewer for the suggestion. We have added a table for comparison with other different forms of TiO_2. It is shown below.

The photocatalytic performance of the prepared fibers in this work is compared with the different forms of other authors, as shown in Table 4. It can be seen that the prepared fibers have better degradation efficiency relative to the recent literature review on TiO_2 photocatalysts.

Table 4 The recent literature review on TiO_2 and the comparison between their photocatalytic efficiency and the results in this work.

Methods	**Photocatalysts type**	**Simulated pollutant**	**The degradation rate constant K value**	**Ref**
Plasma spraying	Coating	Methylene blue	0.0014 min^{-1}	[57]
DBD	Coating	Methyl orange	0.0146 min^{-1}	[58]
Sol-gel method	Particles	Methyl red	0.0160 min^{-1}	[59]
Reactive plasma	Powder	Bacteria	0.0010 min^{-1}	[60]
Hydrothermal synthesis	Fiber	CO_2	0.0110min^{-1}	[61]
DBD	Coating	Methylene blue	0.0099 min^{-1}	[62]
*Electrospinning, calcination	Fiber	Methyl orange	0.0157 min^{-1}	/
*H_2 plasma treatment	Fiber	Methyl orange	0.0223 min^{-1}	/

(DBD: Dielectric Barrier Discharge; * Represents the photocatalysts synthesized in this study)